

Metabolic kinetics of pulmonary surfactant in newborn infants using endogenous stable isotope techniques

Kajsa Bohlin,^{1,*} Bruce W. Patterson,^{1,§} Kimberly L. Spence,^{*} Assaad Merchak,^{*} James C. G. Zozobrado,^{*} Luc J. I. Zimmermann,^{**} Virgilio P. Carnielli,^{††} and Aaron Hamvas^{2,*}

Division of Newborn Medicine,^{*} Edward Mallinckrodt Department of Pediatrics, Washington University School of Medicine and St. Louis Children's Hospital, St. Louis, MO; Division of Pediatrics,[†] Karolinska University Hospital Huddinge and the Karolinska Institute, Stockholm, Sweden; Center for Human Nutrition,[§] Department of Internal Medicine, Washington University School of Medicine, St. Louis, MO; Division of Neonatology,^{**} Maastricht University, Maastricht, The Netherlands; and Division of Neonatal Medicine,^{††} Ospedale Salesi, Ancona, Italy

Abstract We compared kinetic indices of pulmonary surfactant metabolism in premature infants (n = 41) with respect to *i*) tracer ([1-¹³C₁]acetate, [U-¹³C₆]glucose, and [1,2,3,4-¹³C₄] palmitate), *ii*) phospholipid (PL) pool (total PLs or disaturated PLs), or *iii*) instrumentation [gas chromatography/mass spectrometry (GC/MS) or GC-combustion-isotope ratio mass spectrometry (GC-C-IRMS)]. Tracer incorporation was measured in PLs extracted from serial tracheal aspirates after a 24 h tracer infusion. The fractional catabolic rate (FCR), representing the total fractional turnover from all sources of surfactant production, was independent of tracer. The fractional synthesis rate of surfactant PL from plasma palmitate was significantly higher than that from palmitate synthesized de novo from acetate, and these two sources of palmitate together accounted for only half of the total surfactant production in preterm infants. [U-¹³C₆]glucose showed significant recycling of the ¹³C label in intermediary metabolism, distinguishable by GC-MS but not by GC-C-IRMS, resulting in a slower apparent FCR when GC-C-IRMS was used. The extracted PL pool did not affect the surfactant metabolic indices. **■** We suggest that FCR should be used as a primary measure of surfactant turnover kinetics and that tracers labeling both de novo synthesis (acetate and glucose) and preformed pathways (plasma palmitate) can be used to partition the fractional contribution of each pathway to total production.—Bohlin, K., B. W. Patterson, K. L. Spence, A. Merchak, J. C. G. Zozobrado, L. J. I. Zimmermann, V. P. Carnielli, and A. Hamvas. **Metabolic kinetics of pulmonary surfactant in newborn infants using endogenous stable isotope techniques.** *J. Lipid Res.* 2005. 46: 1257–1265.

Supplementary key words acetate • palmitate • mass isotopomer distribution analysis • turnover

The pulmonary surfactant is a phospholipid (PL)-protein complex synthesized and secreted by alveolar type II

cells to maintain alveolar expansion at end expiration. Pulmonary surfactant is composed of ~80% PL, with palmitate constituting ~60–80% of the fatty acid composition. Infants born prematurely have a quantitative deficiency in surfactant that may result in respiratory distress syndrome (1–3). In animal studies, radioactively labeled tracers have been used to determine rates of surfactant synthesis and turnover (3–5). In recent years, the development of stable isotope techniques has enabled human studies and provided a means to better understand the dynamics of lung surfactant metabolism under different physiological conditions.

Several approaches have been used to measure surfactant PL metabolic kinetics in newborn human infants (6–18), pigs (19–21), and baboons (22, 23) using stable isotopically labeled tracers that are incorporated into lung surfactant PL via intravenous administration and new synthesis (endogenously) or via airway administration (exogenously). The methodological details of these approaches show significant differences. Various tracers have been used to endogenously label surfactant PL, including [¹³C]glucose (6, 9–11, 13, 22) or [¹³C]acetate (15, 19–21) to label acetyl-CoA, which in turn labels de novo synthesized palmitate, and labeled palmitate or other fatty acid tracers (7, 12, 14, 18–21) that are incorporated directly into PL (**Fig. 1**). As a result, different precursor pools have been used to calculate the fractional synthesis rate (FSR) of surfactant PL, including plasma glucose (6, 9, 10, 13, 22), plasma fatty acids (7, 12, 14, 18–21), and acetyl-CoA using mass isotope

Abbreviations: DSPL, disaturated phospholipid; FCR, fractional catabolic rate; FSR, fractional synthesis rate; GC-C-IRMS, gas chromatography-combustion-isotope ratio mass spectrometry; MIDA, mass isotopomer distribution analysis; PC, phosphatidylcholine; PL, phospholipid; T_{1/2}, half-life; TTR, tracer-to-tracee ratio.

¹ K. Bohlin and B. W. Patterson contributed equally to this work.

² To whom correspondence should be addressed.

e-mail: hamvas@kids.wustl.edu

Manuscript received 7 December 2004 and in revised form 8 February 2005.

Published, JLR Papers in Press, March 16, 2005.

DOI 10.1194/jlr.M400481-JLR200

Copyright © 2005 by the American Society for Biochemistry and Molecular Biology, Inc.

This article is available online at <http://www.jlr.org>

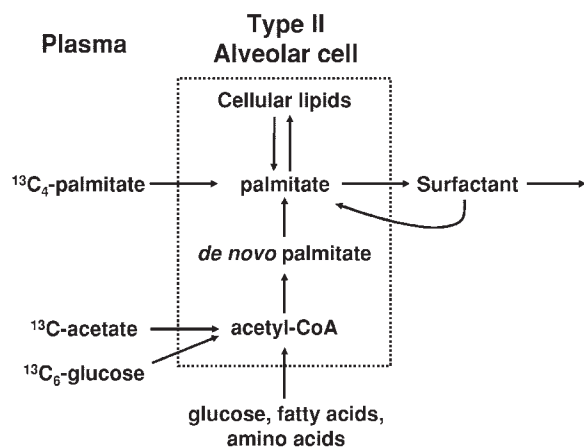


Fig. 1. Pathways for endogenous isotopic labeling of palmitate for surfactant production.

pomer distribution analysis (MIDA) (11, 15, 19–21). In addition, stable isotopically labeled phosphatidylcholines (PCs) have been administered via the airway to label the surfactant pool exogenously (8, 16–18, 23, 24). Furthermore, variations in sample processing techniques have resulted in the analysis of different subfractions of surfactant PL, including total PC (6, 7, 9, 10, 12, 13, 19–24), disaturated PC (8, 14, 16–18), and disaturated phospholipid (DSPL) (11, 15). Finally, different instrumentation has been used to measure stable isotopic enrichment, including gas chromatography-combustion-isotope ratio mass spectrometry (GC-C-IRMS) (6, 7, 9, 10, 13, 18, 22) and GC-MS (8, 11, 12, 14–17, 19–21, 23).

It is unclear to what extent these variations in experimental technique may affect the determination of lung surfactant metabolic parameters. In this report, we systematically examine many of these experimental variables by reanalyzing samples from previously published studies along with recently acquired samples to compare different tracers, some of which were administered simultaneously, to compare different means of processing lung surfactant PL for analysis, and to compare GC-C-IRMS versus GC-MS for the analysis of samples. In addition, we also present a theoretical framework that demonstrates that the FSR depends on the choice of tracer and precursor pool enrichment and that the FSR from any given precursor underestimates the total surfactant turnover rate [fractional catabolic rate (FCR)].

METHODS

Study populations

Infants admitted to the Neonatal Intensive Care Unit at St. Louis Children's Hospital were eligible if they required mechanical ventilation. Infants who were anticipated to require less than 5 days of mechanical ventilation, those with chromosomal anomalies, or those with imminent death were excluded. All medical care, including ventilatory and nutritional management, was determined by the infant's medical team. Written parental informed consent was obtained. The Washington University Human Studies Committee approved the study.

Tracer studies. To compare surfactant precursor incorporation using different tracers, two groups of preterm infants with respiratory distress syndrome were studied with different tracer infusion protocols. Because surfactant administration and nutritional intake may expand the pool of unlabeled precursor, studies were designed to minimize the confounding influences of these therapeutic interventions. All infants received one to two doses of exogenous surfactant replacement within the first 24 h of birth and underwent tracer infusions between 26 and 72 h of age. The composition and amount of nutritional supplementation remained constant during the infusion. No subjects received surfactant replacement after the start of the study. Ventilatory management was not controlled because we had shown previously that ventilatory strategy did not influence the kinetic measures of surfactant metabolism (13).

For the acetate group ($n = 13$), all infants received simultaneous infusions of $[1-^{13}\text{C}]$ acetate and $[1,2,3,4-^{13}\text{C}_4]$ palmitate. Because of unreliable measurements of plasma palmitate enrichment, values of FSR from plasma palmitate were available for only 10 infants.

For the glucose group ($n = 19$), all infants received $[U-^{13}\text{C}_6]$ glucose. The FSR from plasma glucose of total surfactant PC, analyzed by GC-C-IRMS, was previously published for this group (13). The fatty acid methyl esters that were isolated from these samples were reanalyzed by GC-MS for the present report (see below), thereby allowing a distinction between labeled isotopomers and analysis by MIDA. The kinetic analysis was extended to include the FCR, and indices of surfactant metabolism were compared for the different tracers.

The subject characteristics are shown in **Table 1**. Despite the similar gestational ages between the two groups, the mean birth weight of the acetate group was greater than that of the glucose group. The acetate group also underwent tracer infusion an average of 30 h later. There were no differences in the severity of disease or in nutrient intake at the time of the study.

Surfactant PL pools. To compare the effects of PL processing methods (i.e., total PL vs. DSPL) on surfactant metabolic indices, samples from 12 infants were split and analyzed in a paired manner. All infants underwent infusions of $[1-^{13}\text{C}]$ acetate: three of the preterm infants from the acetate group described above and nine older preterm infants of <34 weeks gestation at birth studied between 2 weeks and 2 months of age.

GC-MS versus GC-C-IRMS. To compare mass spectrometry instrumentation, the 19 samples from the glucose group described above, analyzed previously by GC-C-IRMS, were reanalyzed by GC-MS.

Infusion protocol and sample collection

All infants received a 24 h continuous intravenous infusion of tracer. Three tracers were used: $[1-^{13}\text{C}_1]$ acetate (Cambridge Isotope

TABLE 1. Subject characteristics

Variable	Acetate/Palmitate ($n = 13$)	Glucose ($n = 19$)	<i>P</i>
Birth weight (g)	874 ± 49	757 ± 33	0.05
Gestational age (weeks)	26 ± 0.4	26 ± 0.3	0.42
Age at start of study (h)	56 ± 5	26 ± 2	<0.001
Severity score	4.0 ± 0.6	4.3 ± 0.5	0.73
Fat (g/kg/day)	1.4 ± 0.2	1.2 ± 0.3	0.57
Protein (g/kg/day)	1.5 ± 0.2	1.4 ± 0.3	0.72
Total caloric intake/day	42 ± 6	42 ± 3	0.94
Sex (male/female)	7/6	13/6	0.40
Race (white/black/other)	4/7/2	7/12/0	0.21
Mortality (n , [%])	0	6 [32]	0.06

Values shown are means ± SEM.

Laboratories, Inc., Andover, MA) as the sodium salt dissolved in 5% or 10% dextrose, administered at a rate of 120 $\mu\text{mol/kg/h}$ (15); [1,2,3,4- $^{13}\text{C}_4$]palmitate (Isotec, Miamisburg, OH) as the potassium salt bound to human serum albumin, administered at a rate of 2.4 $\mu\text{mol/kg/h}$; and [$U\text{-}^{13}\text{C}_6$] glucose (Campro Scientific, Veenendaal, The Netherlands, and Cambridge Isotope Laboratories) dissolved at 20 mg/ml in 5% or 10% dextrose, infused at a rate of 50 $\mu\text{mol/kg/h}$ labeled glucose (13).

In all studies, fluid and sodium intake were adjusted to maintain preinfusion rates. The start of the study was defined by the start of the tracer infusion. Tracheal aspirates were collected in a standardized manner before the tracer infusion began (time 0) and every 6–12 h for 14 days or until infants were extubated. The tracheal aspirate samples were frozen at -70°C immediately after acquisition. Samples containing visible blood were not included. In infants receiving glucose or palmitate tracers, plasma samples (0.5 ml) were obtained before tracer administration and at ~ 6 h intervals during the 24 h infusion period for the measurement of plasma glucose or palmitate enrichment. Blood was collected in EDTA tubes and centrifuged immediately at 4°C , and plasma was stored at -70°C until processing.

Analytical procedures

The DSPL subfraction of surfactant was isolated from tracheal aspirates from studies in the acetate group as described previously in detail (11, 13, 15). Briefly, tracheal aspirates were thawed and centrifuged to remove cellular debris. For quantification, 101 nmol of internal standard (diheptadecanoylphosphatidylcholine, C17:0-PC; Sigma, St. Louis, MO) was added, and lipids were extracted with chloroform-methanol. Osmium tetroxide was added to the supernatant to form a complex with the unsaturated PLs, and PLs containing only saturated fatty acids were recovered from a column of neutral alumina. To compare DSPL with total PL, samples were split in half after the lipid extraction step; DSPL was recovered from one portion as described, and total PL was recovered from the other portion by omission of osmium tetroxide. Samples from studies in the glucose group were processed previously to yield total PC by thin-layer chromatography (13).

Fatty acid methyl esters were prepared from PL by adding acetyl chloride in methanol and incubating at 70°C for 30 min (11). Methyl esters of plasma fatty acids were prepared as described (25) for the determination of plasma [$^{13}\text{C}_4$]palmitate enrichment.

The fatty acid species in surfactant and plasma fatty acid methyl ester samples were quantified by gas chromatography using a model 5890 system (Hewlett-Packard, Palo Alto, CA) equipped with an Omegawax 320 capillary column (30 m \times 0.32 mm; Supelco, Bellefonte, PA) and a flame ionization detector, using the C17:0 peak as an internal standard. The isotopic enrichment of methyl palmitate from surfactant and plasma was measured by GC-MS (model 5973; Hewlett-Packard) using a 30 m \times 0.25 mm DB-5 column as described (25). Enrichment is expressed as tracer-to-tracee ratio (TTR), representing the molar ratio of labeled to unlabeled palmitate in the sample. Samples from studies in the glucose group were analyzed previously by GC-C-IRMS with correction for the contribution of unlabeled carbon atoms added during derivatization (13). For the present report, the fatty acid methyl ester samples were recovered from the freezer where they had been stored after the GC-C-IRMS analysis, redissolved in heptane, and reanalyzed by GC-MS as described above. The time points analyzed for each study were identical between the two instrumentation modalities.

Kinetic analysis

Indices of surfactant metabolism were determined from each individual isotopic enrichment time course. These included the

time of appearance of tracer in the surfactant palmitate (in hours) (13), the FSR (i.e., the percentage of the surfactant pool synthesized from a given precursor per day), the FCR (i.e., the percentage of the surfactant pool removed and replaced by newly produced material per day), and the FSR/FCR ratio, which represents the contribution of newly synthesized surfactant from a given precursor to total surfactant turnover (see below).

Figure 2 illustrates the principles used to analyze surfactant kinetics. The kinetic analysis assumes the system is at steady state, so that the rates of formation (FSR) and breakdown (FCR) of surfactant are constant. First, consider a precursor-product relationship (Fig. 2A) in which an isotopically labeled precursor is the

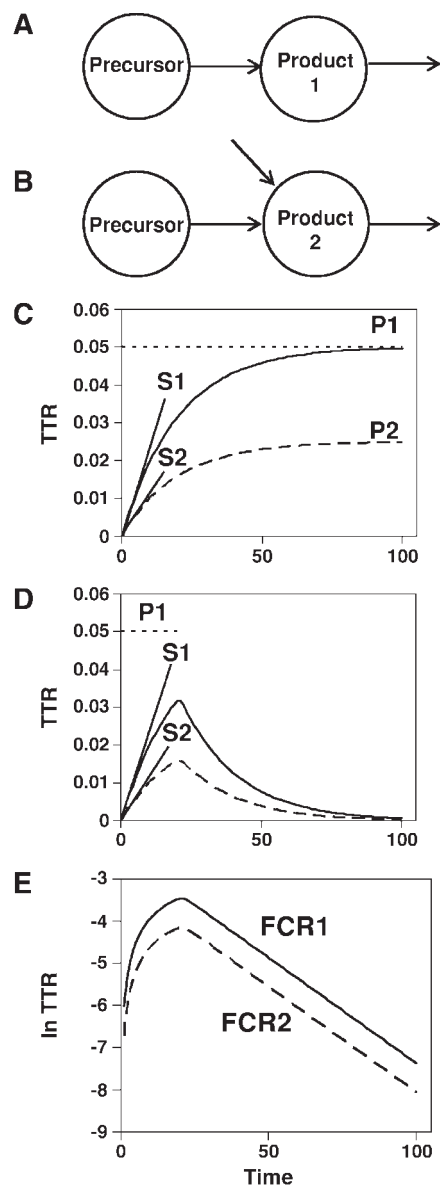


Fig. 2. Principles of kinetic analysis. A and B: Exclusive and non-exclusive precursor-product relationships, respectively. C: Rise-to-plateau kinetics for product 1 (solid line) and product 2 (dashed line). P1 and P2 represent plateaus for products 1 and 2; S1 and S2 represent initial linear slopes for the two curves. D: Same conditions, except the tracer infusion is shortened. E: Same data as in D after taking natural logarithms. Fractional catabolic rates (FCR1 and FCR2) are calculated from the negative of the monoexponential slopes of the descending curves. TTR, tracer-to-tracee ratio.

exclusive precursor for a given product. Given an appropriate infusion of tracer, a constant precursor enrichment can be achieved (Fig. 2C, plateau P1, dotted line). If the tracer infusion is of sufficient duration, the product will ultimately achieve the enrichment of this precursor (Fig. 2C, solid curve; initial linear slope = S1, plateau = P1). The FSR for the product = initial linear slope S1 ÷ plateau P1 (26); this FSR corresponds to the total FCR of the product, because plateau P1 represents the only precursor for the product.

Next, consider that another pathway exists for product formation that is not labeled by the applied tracer, which causes isotopic dilution distal to the precursor enrichment P1 (Fig. 2B). For this illustration, the rate of input of unlabeled material was set equal to the rate of input of labeled precursor, so that at all times the enrichment of the product is one-half that of the former case. With a sufficiently long tracer infusion, the product will achieve a plateau enrichment (Fig. 2C, dashed line; initial linear slope = S2, plateau = P2) that is one-half of precursor plateau P1. If the ultimate plateau P2 is known, FSR = initial linear slope S2 ÷ P2 will give the same result as in the former case, because isotopic dilution affects all time points equally and P2 represents the final plateau in the product after accounting for isotopic dilution of the precursor. However, if precursor plateau P1 (before isotopic dilution) is used rather than P2, then FSR_{P1} = S2 ÷ P1 will underestimate the true FCR. Here, the subscript signifies that only one of perhaps several production pathways was traced, and this formula recognizes that isotopic dilution has occurred distal to the precursor pool whose enrichment was used for the FSR calculation. The ratio FSR_{P1} ÷ FCR will equal the fraction of the total production that arose from the precursor pathway of P1 enrichment (50% in this illustration).

If the duration of tracer infusion is decreased, the product enrichment will increase to a peak and then return toward baseline (Fig. 2D). The initial increase in enrichment is unaltered, so S1 and S2 will be the same as in Fig. 2C. The decrease in enrichment is monoexponential (Fig. 2E) if the product is kinetically homogeneous and there is no appearance of tracer in the product after the tracer infusion is halted. The monoexponential slope is unaffected by isotopic dilution distal to the precursor plateau P1. The FCR is calculated as the negative of the monoexponential slope and corresponds to the total fractional turnover rate in pools per unit of time (or alternatively, the total FSR) because it represents the replacement of tracer-labeled product with unlabeled product from all production pathways, whether or not they were initially labeled with tracer. Half-life ($T_{1/2}$) is calculated as $T_{1/2} = \ln 2 / \text{FCR}$.

MIDA can be used to measure the FSR of surfactant from de novo synthesized palmitate derived from the rate of incorporation of labeled acetate or glucose (11, 19, 26). Briefly, acetyl-CoA precursor enrichment is determined by the ratio of doubly to singly labeled palmitate (corresponding to the incorporation of two and one labeled acetate subunits, respectively). When [^{13}C]acetate is used, singly and doubly labeled palmitate correspond to the $m+1$ and $m+2$ isotopomers, respectively, and when [$^{13}\text{C}_6$]glucose is used, they correspond to the $m+2$ and $m+4$ isotopomers, respectively, because [$1,2\text{-}^{13}\text{C}_2$]acetate is produced from the starting tracer. The FSR from de novo synthesized palmitate (FSR_{acetate}) is determined from the rate of change of enrichment of $m+1$ (for [^{13}C]acetate) or $m+2$ (for [$^{13}\text{C}_6$]glucose) and the plateau enrichment of newly synthesized palmitate as determined by MIDA (27). This FSR will underestimate FCR because there is isotopic dilution distal to the de novo synthesized palmitate pool (Figs. 1, 2).

To measure the FSR from plasma palmitate, the average enrichment of [$^{13}\text{C}_4$]palmitate in plasma ($\text{TTR}_{p(m+4)}$) is obtained over the 24 h infusion period. The FSR from plasma palmitate is

calculated from the rate of change of enrichment of $(m+4)$ -labeled palmitate in surfactant:

$$\text{FSR}_{\text{palmitate}} = \frac{(\Delta \text{TTR}_{m+4} / \Delta t)}{\text{TTR}_{p(m+4)}} \quad (\text{Eq. 1})$$

Again, this expression underestimates the total FCR because there is isotopic dilution distal to the plasma palmitate pool (cf. Figs. 1, 2).

In our previous study (13) using the [$^{13}\text{C}_6$]glucose tracer, the FSR from plasma glucose was calculated as

$$\text{FSR}_{\text{glucose}} = \frac{(\Delta E_{\text{palmitate}} / \Delta t)}{E_{p(\text{glucose})}} \quad (\text{Eq. 2})$$

where the enrichments (E) for surfactant palmitate and plasma glucose were measured as atomic enrichments of carbon after combustion to CO_2 . This expression thus literally calculates the fraction of surfactant palmitate carbon derived from plasma glucose carbon per unit of time. Once again, this expression underestimates the total FCR because there is isotopic dilution from other substrates contributing carbon to the acetyl-CoA pool in addition to sources of palmitate other than de novo synthesis (cf. Figs. 1, 2).

Statistical analyses

Results shown are means \pm SEM. Two-tailed Student's t -tests were used for normally distributed data, Mann-Whitney U -tests for nonnormally distributed data, Chi-square and Fisher's exact tests for categorical data, Pearson coefficients for correlation analysis, and paired-samples t -tests for paired data. Linear regression models were also used to determine the influences of covariates, as specified. Statistical analyses were performed using the Statistical Analysis System (SAS version 8.1; SAS Institute, Cary, NC) and SPSS version 11.5 (SPSS, Inc., Chicago, IL).

RESULTS

Tracer studies

A typical time course for [^{13}C]acetate and plasma [$^{13}\text{C}_4$] palmitate incorporation into lung surfactant DSPL palmitate for a preterm infant is illustrated in **Fig. 3**. The greatest enrichment is observed for palmitate that has incorporated a single [^{13}C]acetate ($m+1$ palmitate), with decreasing enrichment of palmitate that has incorporated two or three labeled acetates ($m+2$, $m+3$; Fig. 3A, B). Based on the isotopomer distribution of $m+1$, $m+2$, and $m+3$ palmitate, a trivial enrichment of $m+4$ palmitate from the incorporation of four labeled acetates is expected (0.01–0.02%). Figure 3B shows substantial enrichment of $m+4$ palmitate as a result of the incorporation of plasma [$^{13}\text{C}_4$] palmitate. The initial linear slopes of $m+1$ and $m+4$ palmitate are used to calculate FSR_{acetate} and FSR_{palmitate}, respectively. The $m+2/m+1$ isotopomer ratio is constant over the major portion of the peak (Fig. 3C), from which the precursor acetyl-CoA enrichment is determined by MIDA. The FCR is calculated from the downslope of the time-enrichment curve after peak enrichment (Fig. 3D). This downslope is typically monoexponential for all isotopomers, $m+1$ through $m+4$.

A typical time course for [$^{13}\text{C}_6$]glucose incorporation into surfactant palmitate is shown in **Fig. 4**. The greatest

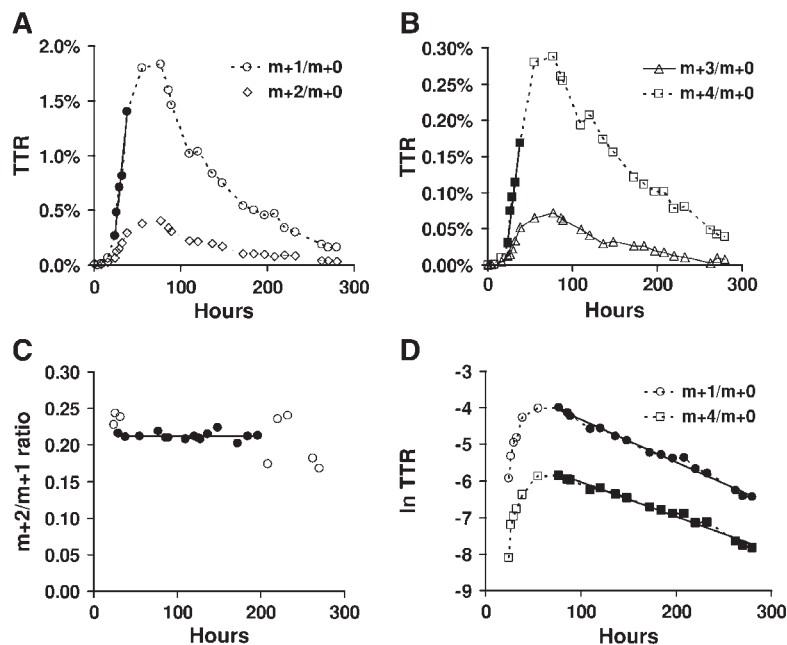


Fig. 3. Time course for tracer incorporation into lung surfactant palmitate after a 24 h infusion of $[1\text{-}^{13}\text{C}]$ acetate and $[^{13}\text{C}_4]$ palmitate. A and B: TTRs for m+1, m+2, and m+3 palmitate (from incorporation of one to three labeled acetate subunits) and m+4 palmitate (from incorporation of plasma $[^{13}\text{C}_4]$ palmitate). Note the difference in y axis scales. Closed symbols and regression lines indicate upslopes used to calculate fractional synthesis rates $[\text{FSR}_{\text{acetate}}$ (m+1 data) and $\text{FSR}_{\text{palmitate}}$ (m+4 data)]. C: Ratio of doubly to singly labeled palmitate from acetate incorporation. Closed symbols show points selected to calculate the average ratio of doubly to singly labeled palmitate. D: Natural log transform of the m+1 and m+4 TTRs. Closed symbols and regression lines show slopes used to calculate FCR.

enrichment is observed for m+2 palmitate, corresponding to the incorporation of a single $[1,2\text{-}^{13}\text{C}_2]$ acetate subunit (Fig. 4A). Palmitate that has incorporated two acetate subunits is also formed (m+4; Fig. 4B). The m+4/m+2 ratio, from which the acetyl-CoA enrichment is determined, is constant (Fig. 4C). The monoexponential slopes of m+2 and m+4 palmitate are parallel (Fig. 4D). Substantial enrichment is also observed for m+1 palmitate, which corresponds to the incorporation of one singly labeled acetate subunit arising from the recycling of carbon skeletons through pathways of intermediary metabolism. The substantially slower monoexponential slope of (m+1)-labeled palmitate demonstrates this tracer recycling (Fig. 4D). Enrichment is virtually undetectable for m+3 palmitate, arising from the incorporation of one doubly and one singly labeled acetate (Fig. 4B).

Kinetic parameters are summarized in **Table 2**. The FCR, representing the total fractional turnover rate (or total FSR), was not significantly different regardless of which tracer was used. In the infants who received simultaneous infusions of $[^{13}\text{C}]$ acetate and $[^{13}\text{C}_4]$ palmitate, the FSR from plasma palmitate was significantly higher than the FSR from acetate (de novo synthesized palmitate). Thus, the fractional contribution of plasma palmitate to total surfactant production ($\text{FSR}_{\text{palmitate}}/\text{FCR}$) was also greater than the contribution of de novo synthesized palmitate to surfactant production ($\text{FSR}_{\text{acetate}}/\text{FCR}$). Together, $(\text{FSR}_{\text{acetate}} + \text{FSR}_{\text{palmitate}})/\text{FCR}$ accounted for only $\sim 50\%$ of the total surfactant turnover. Using MIDA, the FSR from acetate was similar for the two groups that received either $[^{13}\text{C}]$ acetate or $[\text{U-}^{13}\text{C}_6]$ glucose. Numerically, the values for FSR and FCR diverged, so that the FSR/FCR ratio for the ace-

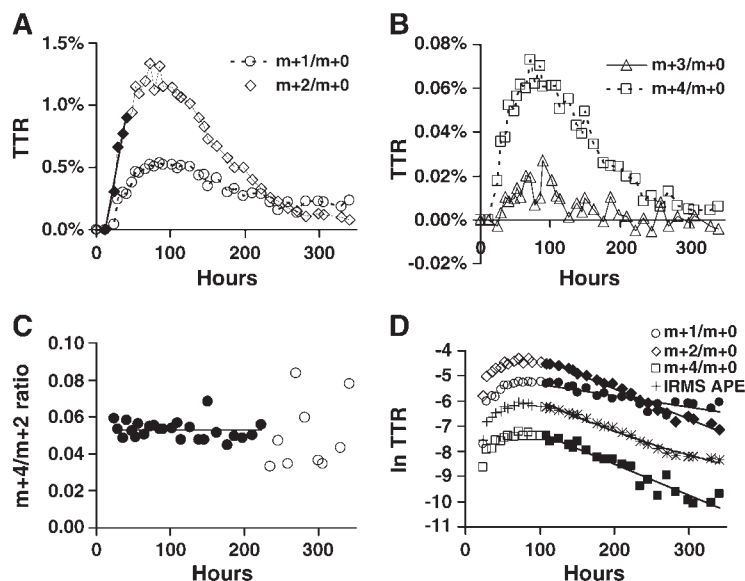


Fig. 4. Time course for tracer incorporation into lung surfactant palmitate after a 24 h infusion of $[\text{U-}^{13}\text{C}_6]$ glucose. A and B: TTRs for m+1, m+2, m+3, and m+4 palmitate (note the difference in y axis scales). Closed symbols and regression lines indicate upslopes used to calculate $\text{FSR}_{\text{acetate}}$. C: Ratio of doubly to singly labeled palmitate from acetate incorporation. Closed symbols show points selected to calculate the average ratio of doubly to singly labeled palmitate. D: Natural log transform of the m+1 (circles), m+2 (diamonds), and m+4 (squares) TTRs. FCR is calculated from the indicated slope of m+2 atom (closed diamonds). Also included are log values of the ^{13}C atom percent excess of the same samples measured by gas chromatography-combustion-isotope ratio mass spectrometry (IRMS APE; plus signs).

TABLE 2. Surfactant kinetics in preterm infants

Variable	[¹³ C ₄]palmitate (n = 13)	[1- ¹³ C]acetate (n = 13)	[U- ¹³ C ₆]glucose ^a (n = 19)	P
FCR (% pools/day)	23.5 ± 1.7	26.3 ± 1.9	23.4 ± 1.8	0.48 ^b
FSR _{acetate} (MIDA) (% pools/day)		4.9 ± 0.8	6.0 ± 0.6	0.28
FSR _{palmitate} (% pools/day)	7.4 ± 1.6 ^c			0.02 ^d
FSR _{acetate} /FCR (%)		18.5 ± 2.6	28.5 ± 3.7	0.05
FSR _{palmitate} /FCR (%)	28.9 ± 6.1 ^c			0.02 ^d
Time of appearance of tracer (h)	14.7 ± 2.0	15.2 ± 1.8	16.2 ± 1.3	0.79

Values shown are means ± SEM. FCR, fractional catabolic rate; FSR, fractional synthesis rate; MIDA, mass isotope distribution analysis.

^a Results from the GC-MS and MIDA analyses.

^b ANOVA.

^c FSR values available for n = 10.

^d Paired *t*-test, FSR_{acetate} (from [1-¹³C]acetate) versus FSR_{palmitate}.

tate group was less than that for the glucose group ($P = 0.052$). A linear regression model incorporating the significant differences between the two groups in birth weight or age at the start of the study with univariate analysis did not reveal any significant independent influences from these factors. The time of first appearance in surfactant palmitate for each of the tracers was not significantly different.

Surfactant PL pool for sample processing

The quantity of PL recovered from tracheal aspirates was constant across time for virtually all studies (data not shown). The quantity of recovered PL, fatty acid composition, and surfactant kinetics indices were compared in paired samples processed with (DSPL) and without (total PL) osmium tetroxide. The amount of PL isolated from tracheal aspirates was 2-fold higher in total PL samples compared with DSPL samples (213 ± 37 nmol and 112 ± 22 nmol in total PL and DSPL, respectively; $P < 0.001$). In total PL samples, the fatty acid composition showed a significantly lower proportion of palmitate than in DSPL samples, attributable to the presence of palmitoleate, oleate, and linoleate ($58 \pm 2\%$ and $81 \pm 3\%$ palmitate in total PL and DSPL, respectively; $P < 0.001$). However, the surfactant metabolic indices for acetate incorporation (FCR, FSR_{acetate}, FSR_{acetate}/FCR, and acetyl-CoA precursor enrichment) were not significantly different for total PL compared with DSPL (data not shown), suggesting that the surfactant and nonsurfactant PL pools were turning over at the same rate or that the palmitate extracted from the tracheal aspirates was derived primarily from the surfactant pool.

GC-MS versus GC-C-IRMS

There were no differences in the indices of surfactant metabolism between the instruments, except for FCR ($23.4 \pm 1.8\%$ and $21.1 \pm 1.5\%$ pools/day for GC-MS and GC-C-IRMS, respectively; $P < 0.01$ by paired *t*-test). This was explained by an increase of the m+1 enrichment at the tail end of the time-enrichment curve, as detected by GC-MS and described above (Fig. 4A). At the peak of m+2 palmitate enrichment, the m+1 fraction represented $28 \pm 5\%$ of detectable enrichment from all isotopomers; however, at the tail it contributed $52 \pm 15\%$ and

actually equaled or exceeded the m+2 enrichment ($P = 0.001$). The increase in m+1 in the tail contributes to a consistent underestimation of the decrease in palmitate enrichment and apparently lower FCR when [U-¹³C₆]glucose is used as a tracer and palmitate enrichment is measured by GC-C-IRMS, which cannot distinguish between the different mass species (Fig. 4D).

DISCUSSION

In this report, we describe and compare several approaches that have been used to evaluate the metabolic kinetics of lung surfactant PL using stable isotopically labeled tracers that are incorporated endogenously. We have focused on the palmitate fraction in all our comparisons, because it constitutes ~60% of the fatty acids in total surfactant PLs.

Approaches to measuring metabolic kinetics

We (13, 15) and others (6, 7, 9, 12, 14, 22) have previously used certain descriptive parameters (the time to maximum enrichment and the maximum enrichment) to assess surfactant kinetics. Although useful for making comparisons between groups, these parameters lack physiological significance. In contrast, the monoexponential slope FCR simultaneously quantifies surfactant turnover and encapsulates these descriptive parameters (note that faster FCR results in higher maximum enrichment and shorter time to maximum enrichment parameters, all else being equal). If it is assumed that there is no further tracer incorporation during the downslope, all newly produced surfactant will be unlabeled and will dilute the isotopic enrichment of previously labeled surfactant. The monoexponential slope FCR thus measures the total fractional turnover rate from all sources of surfactant production, regardless of which pathway(s) was initially labeled with tracer. Indeed, the FCRs measured using [U-¹³C₆]glucose, [1-¹³C]acetate, and [¹³C₄]palmitate were not significantly different (Table 2), suggesting that each tracer is interrogating the same pool. Because FSR from individual labels accounts for only a proportion of the total surfactant turnover, we propose that the FCR, which actually is the total FSR, should be

used as a primary measure of surfactant turnover kinetics. If desired, $T_{1/2}$ may be determined from FCR. To measure FCR, taking the natural log values and selecting points that fall on a straight line (Figs. 3D, 4D) provides an easier and less subjective means of curve fitting than attempting to determine the points with which to fit an exponential function (7–9, 15).

FCR represents the total fractional surfactant production rate. By providing tracers for the biosynthetic pathway ($[U-^{13}C]$ glucose, $[^{13}C]$ acetate) and plasma fatty acids ($[^{13}C_4]$ palmitate), we were able to partition the fractional contribution of each of these pathways to total production. By difference, we can discern the fraction of production coming from other sources that were not labeled with these tracers. Some of this unlabeled production may come from turnover of tissue lipid components or plasma triglycerides. Studies in rabbits have demonstrated that ~90% of the surfactant pool is recycled in newborns and 50% is recycled in adults (28, 29). Thus, if a similar situation exists in humans, it is likely that a significant proportion of this new production may come from recycling of lung surfactant itself (Fig. 1). Full resolution of this matter will require simultaneous application of distinctly labeled endogenous and exogenous tracers.

We have observed that the downslope from peak enrichment is typically monoexponential for both acetate and palmitate tracers (Fig. 3). This is consistent with a system that behaves as a single compartment at metabolic steady state with no tracer recycling, such that all surfactant produced after the peak of enrichment is isotopically unlabeled. Nevertheless, it is possible that tracer recycling may affect the results in such a way that a biexponential peak is not observed. The FCR determined from the monoexponential slope will underestimate the true FCR of surfactant if there is significant tracer recycling (30).

Choice of tracers

The many different tracers that have been used in previous studies may lead to confusion with respect to the various metabolic indices being reported. However, in studies in which the palmitate fraction of the PL is being evaluated, FCR should be the same regardless of tracer. We showed that this is true for $[U-^{13}C]$ glucose, $[^{13}C]$ acetate, and $[^{13}C_4]$ palmitate (Table 2), demonstrating the utility of the FCR as a measure of total surfactant turnover. The difference between tracers lies in the relative contribution of each pathway to total surfactant synthesis. We demonstrated that the flux of plasma palmitate into surfactant PL was higher than that of de novo synthesized palmitate and that together these two sources of palmitate accounted for only half of total surfactant production in preterm infants. Cavicchioli et al. (12) infused $[U-^{13}C]$ palmitate to preterm infants and found FSR from plasma palmitate to be $12 \pm 7.7\%$ /day. This value is higher than our $7.4 \pm 1.6\%$, but the infants in the present study were more immature (26 vs. 28 weeks of gestation), which may explain the difference. In a previous study of a group of premature infants who received $[^{13}C]$ acetate, we reported that $FSR_{acetate}$ was $2.0 \pm 0.4\%$ /day and FCR was $16.8 \pm 1.6\%$ /

day, both of which are significantly different from the values in the current group of infants (15). A linear regression model incorporating the significant differences in birthweight, fat intake, and age at the start of the study between the two groups found that birthweight and age at the start of the study explained the differences in kinetics.

Theoretically, because glucose is converted to acetyl-CoA and therefore labels the same de novo synthesis pathway as acetate, FSR values should be similar for acetate and glucose tracers. Indeed, we found this to be the case when MIDA was used to determine the acetyl-CoA precursor enrichment and surfactant FSR. However, when comparing values in the 19 infants who received $[U-^{13}C_6]$ glucose, the FSR from acetate as determined by MIDA was significantly greater than the FSR from plasma glucose for the 19 infants reported previously in two separate groups (13) ($FSR_{acetate} = 6.0 \pm 0.6\%$ /day with MIDA vs. $FSR_{plasma\ glucose} = 4.5 \pm 0.6\%$ /day; $P = 0.02$ by paired *t*-test). This is expected, because the alveolar acetyl-CoA pool is derived from sources other than plasma glucose (Fig. 1), such that there is isotopic dilution distal to the plasma $[^{13}C_6]$ glucose precursor enrichment (see above). Furthermore, the extent of this isotopic dilution (the ratio $FSR_{plasma\ glucose}/FSR_{acetate}$) suggests that 75% of the acetyl-CoA flux in type II alveolar cells is derived from plasma glucose, which appears reasonable for a newborn primarily on a glucose metabolism economy. Although these differences in FSR values are small in the practical sense, this nevertheless demonstrates that MIDA reliably estimates the enrichment of an otherwise inaccessible precursor compartment and thus provides a more reliable determination of the FSR than does the use of plasma precursor enrichment, which may not be the most appropriate precursor compartment.

In summary, each tracer that has been used in studies of surfactant metabolism can provide insight into that specific precursor utilization. We suggest, however, that using acetate permits the use simultaneous tracers (with $[^{13}C_4]$ palmitate) and also provides greater acetyl-CoA enrichments at lower cost compared with $[U-^{13}C_6]$ glucose.

Surfactant PL pool for sample processing

Because surfactant is enriched in DSPLs, previous studies have assumed that extraction of total PC (6, 7, 9, 10, 12, 13, 19–23), disaturated PC (8, 14, 16–18), or DSPL (11, 15) would yield representative subfractions of surfactant PL. In the face of lung disease, significant amounts of nonsurfactant PL may be present in the airway (e.g., plasma infiltration), which may have a different turnover rate, affecting the indices of surfactant metabolism depending on the specific pool being evaluated. However, the present data showed no significant differences in the metabolic indices of surfactant from samples processed either as DSPL or total PL, in spite of differences in the fatty acid composition and amount of PL in samples. When analyzed by tandem mass spectrometry, DSPL samples contained 89% palmitate, total PL contained 55% palmitate, and total PC contained 62% palmitate (A. Hamvas and F. Hsu, unpublished observations). The PLs of DSPL were 98% PC. Hence, because no differences in surfactant metabolic indices were


found between total PL and DSPL, the similar amounts of palmitate in total PL and PC suggest that the metabolic indices would also be similar for DSPL and total PC and that studies measuring labeled palmitate incorporation into PL can be compared and are valid regardless of which palmitate pool is being interrogated. Note, however, that this argument does not apply when comparing the kinetics of different labeled fatty acids. Cavicchioli et al. (12) observed 2-fold differences in FCR and FSR between [U-¹³C] palmitate and [U-¹³C]linoleate when the two tracers were administered simultaneously. The linoleate tracer cannot appear on a DSPL; thus, the molecular heterogeneity of PL species may have accounted for this difference between fatty acid tracers. Linoleate is the major fatty acid found in PLs originating from cellular debris or plasma, and it is possible that these molecular species may have substantially different kinetics from those of DSPLs that contain most of the palmitate tracer.

GC-MS versus GC-C-IRMS

The enrichment after peak is usually monoexponential until enrichments approach baseline values, when [¹³C] acetate or [¹³C₄]palmitate tracers are used and the samples are analyzed by GC-MS. However, on occasions when there appears to be a contribution of a slower, second exponential term, our bias is to use the earlier monoexponential closer to the peak because a later, slower component is likely to be affected by tracer recycling artifacts. In contrast, Bunt et al. (6) observed biexponential decay when [U-¹³C₆] glucose was used as a tracer and samples were measured by GC-C-IRMS. The later, slower monoexponential term was used to characterize surfactant turnover because the earlier, faster monoexponential may be affected by the incorporation of plasma palmitate that was labeled with ¹³C via hepatic lipogenesis. However, our results suggest that the biexponential appearance observed in those earlier studies likely resulted from using [U-¹³C]glucose and GC-C-IRMS. We have demonstrated that there is significant recycling of the ¹³C label in intermediary metabolism, resulting in the formation of [¹³C₁]acetate that is incorporated into surfactant palmitate, and that the relative contribution of this process increases during the time course (Fig. 4). This recycling of singly ¹³C-labeled acetyl-CoA will attenuate the downslope, thereby creating a biexponential curve when samples are analyzed by GC-C-IRMS. Note that the kinetics are clearly monoexponential when [U-¹³C] glucose is used but samples are analyzed by GC-MS to look exclusively at palmitate that has incorporated one or two [¹³C₂]acetate precursors, whereas the downslope appears biexponential when the samples are analyzed by GC-C-IRMS (Fig. 4D).

Conclusion

Despite using different tracers, instruments, and PL pools, studies using stable isotope methods to study surfactant metabolism arrive at similar numbers and thus can be compared effectively. We have extended those studies to develop the idea that FCR is a primary measure of surfactant turnover kinetics. Labeling of both de novo synthesis (ace-

tate and glucose) and preformed pathways (plasma palmitate) is needed to partition the fractional contribution of each pathway to total production. The addition of intratracheally administered labeled surfactant will expand the ability to estimate surfactant pool sizes and to interrogate the remaining major pathway of surfactant metabolism. 

The authors thank Junyoung Kwon and Freida Custodio for excellent technical assistance, F. Sessions Cole and Mats Blennow for support and scientific advice, Kristina Bryowski for tracer preparation, and the Neonatal Intensive Care Unit staff at St. Louis Children's Hospital for help and sample collection. This work was supported by grants from the Swedish Society of Medicine (to K.B.) and the National Institutes of Health (R01 HL-65385 to A.H., DK-56341 to the Clinical Nutrition Research Unit, and RR-00954 to the Biomedical Mass Spectrometry Resource).

REFERENCES

1. Avery, M. E., and J. Mead. 1959. Surface properties in relation to atelectasis and hyaline membrane disease. *AMA J. Dis. Child.* **97**: 517–523.
2. Malloy, M. H., and D. H. Freeman. 2000. Respiratory distress syndrome mortality in the United States, 1987 to 1995. *J. Perinatol.* **20**: 414–420.
3. Ikegami, M., A. Jobe, and P. W. Nathanielsz. 1981. The labeling of pulmonary surfactant phosphatidylcholine in newborn and adult sheep. *Exp. Lung Res.* **2**: 197–206.
4. Jobe, A., and L. Gluck. 1979. The labeling of lung phosphatidylcholine in premature rabbits. *Pediatr. Res.* **13**: 635–640.
5. Jacobs, H., A. Jobe, M. Ikegami, and S. Jones. 1982. Surfactant phosphatidylcholine source, fluxes, and turnover times in 3-day-old, 10-day-old, and adult rabbits. *J. Biol. Chem.* **257**: 1805–1810.
6. Bunt, J. E., L. J. Zimmermann, J. L. Wattimena, R. H. van Beek, P. J. Sauer, and V. P. Carnielli. 1998. Endogenous surfactant turnover in preterm infants measured with stable isotopes. *Am. J. Respir. Crit. Care Med.* **157**: 810–814.
7. Cogo, P. E., V. P. Carnielli, J. E. Bunt, T. Badon, G. Giordano, F. Zacchello, P. J. Sauer, and L. J. Zimmermann. 1999. Endogenous surfactant metabolism in critically ill infants measured with stable isotope labeled fatty acids. *Pediatr. Res.* **45**: 242–246.
8. Torresin, M., L. J. Zimmermann, P. E. Cogo, P. Cavicchioli, T. Badon, G. Giordano, F. Zacchello, P. J. Sauer, and V. P. Carnielli. 2000. Exogenous surfactant kinetics in infant respiratory distress syndrome: a novel method with stable isotopes. *Am. J. Respir. Crit. Care Med.* **161**: 1584–1589.
9. Bunt, J. E., V. P. Carnielli, J. L. Darcos Wattimena, W. C. Hop, P. J. Sauer, and L. J. Zimmermann. 2000. The effect in premature infants of prenatal corticosteroids on endogenous surfactant synthesis as measured with stable isotopes. *Am. J. Respir. Crit. Care Med.* **162**: 844–849.
10. Bunt, J. E., V. P. Carnielli, D. J. Janssen, J. L. Wattimena, W. C. Hop, P. J. Sauer, and L. J. Zimmermann. 2000. Treatment with exogenous surfactant stimulates endogenous surfactant synthesis in premature infants with respiratory distress syndrome. *Crit. Care Med.* **28**: 3383–3388.
11. Merchak, A., B. W. Patterson, K. E. Yarasheski, and A. Hamvas. 2000. Use of stable isotope labeling technique and mass isotopomer distribution analysis of [(13)C]palmitate isolated from surfactant disaturated phospholipids to study surfactant in vivo kinetics in a premature infant. *J. Mass Spectrom.* **35**: 734–738.
12. Cavicchioli, P., L. J. Zimmermann, P. E. Cogo, T. Badon, G. Giordano, M. Torresin, F. Zacchello, and V. P. Carnielli. 2001. Endogenous surfactant turnover in preterm infants with respiratory distress syndrome studied with stable isotope lipids. *Am. J. Respir. Crit. Care Med.* **163**: 55–60.
13. Merchak, A., D. J. Janssen, K. Bohlin, B. W. Patterson, L. J. Zimmermann, V. P. Carnielli, and A. Hamvas. 2002. Endogenous pulmonary surfactant metabolism is not affected by mode of ventila-

- tion in premature infants with respiratory distress syndrome. *J. Pediatr.* **140**: 693–698.
14. Cogo, P. E., L. J. Zimmermann, F. Rosso, F. Tormena, P. Gamba, G. Verlato, A. Baritussio, and V. P. Carnielli. 2002. Surfactant synthesis and kinetics in infants with congenital diaphragmatic hernia. *Am. J. Respir. Crit. Care Med.* **166**: 154–158.
 15. Bohlin, K., A. Merchak, K. Spence, B. W. Patterson, and A. Hamvas. 2003. Endogenous surfactant metabolism in newborn infants with and without respiratory failure. *Pediatr. Res.* **54**: 185–191.
 16. Cogo, P. E., L. J. Zimmermann, L. Meneghini, N. Mainini, L. Bordinon, V. Suma, M. Buffo, and V. P. Carnielli. 2003. Pulmonary surfactant disaturated-phosphatidylcholine (DSPC) turnover and pool size in newborn infants with congenital diaphragmatic hernia (CDH). *Pediatr. Res.* **54**: 653–658.
 17. Cogo, P. E., L. J. Zimmermann, R. Pesavento, E. Sacchetto, A. Burighel, F. Rosso, T. Badon, G. Verlato, and V. P. Carnielli. 2003. Surfactant kinetics in preterm infants on mechanical ventilation who did and did not develop bronchopulmonary dysplasia. *Crit. Care Med.* **31**: 1532–1538.
 18. Cogo, P. E., L. J. Zimmermann, G. Verlato, P. Midrio, A. Gucciardi, C. Ori, and V. P. Carnielli. 2004. A dual stable isotope tracer method for the measurement of surfactant disaturated-phosphatidylcholine net synthesis in infants with congenital diaphragmatic hernia. *Pediatr. Res.* **56**: 184–190.
 19. Martini, W. Z., D. L. Chinkes, R. E. Barrow, E. D. Murphey, and R. R. Wolfe. 1999. Lung surfactant kinetics in conscious pigs. *Am. J. Physiol.* **277**: E187–E195.
 20. Martini, W. Z., O. Irtun, D. L. Chinkes, R. E. Barrow, and R. R. Wolfe. 2000. Glucose effects on lung surfactant kinetics in conscious pigs. *Am. J. Physiol. Endocrinol. Metab.* **279**: E920–E926.
 21. Martini, W. Z., O. Irtun, D. L. Chinkes, R. E. Barrow, and R. R. Wolfe. 2001. Surfactant phosphatidylcholine in thermally injured pigs. *Crit. Care Med.* **29**: 1417–1422.
 22. Bunt, J. E., V. P. Carnielli, S. R. Seidner, M. Ikegami, J. L. Darcos Wattimena, P. J. Sauer, A. H. Jobe, and L. J. Zimmermann. 1999. Metabolism of endogenous surfactant in premature baboons and effect of prenatal corticosteroids. *Am. J. Respir. Crit. Care Med.* **160**: 1481–1485.
 23. Janssen, D. J., V. P. Carnielli, P. E. Cogo, S. R. Seidner, I. H. Luijendijk, J. L. Wattimena, A. H. Jobe, and L. J. Zimmermann. 2002. Surfactant phosphatidylcholine half-life and pool size measurements in premature baboons developing bronchopulmonary dysplasia. *Pediatr. Res.* **52**: 724–729.
 24. Janssen, D. J., D. Tibboel, V. P. Carnielli, E. van Emmen, I. H. Luijendijk, J. L. Darcos Wattimena, and L. J. Zimmermann. 2003. Surfactant phosphatidylcholine pool size in human neonates with congenital diaphragmatic hernia requiring ECMO. *J. Pediatr.* **142**: 247–252.
 25. Patterson, B. W., G. Zhao, N. Elias, D. L. Hachey, and S. Klein. 1999. Validation of a new procedure to determine plasma fatty acid concentration and isotopic enrichment. *J. Lipid Res.* **40**: 2118–2124.
 26. Patterson, B. W. 1997. Use of stable isotopically labeled tracers for studies of metabolic kinetics: an overview. *Metabolism.* **46**: 322–329.
 27. Chinkes, D. L., A. Aarsland, J. Rosenblatt, and R. R. Wolfe. 1996. Comparison of mass isotopomer dilution methods used to compute VLDL production in vivo. *Am. J. Physiol.* **271**: E373–E383.
 28. Jacobs, H., A. Jobe, M. Ikegami, and D. Conaway. 1983. The significance of reutilization of surfactant phosphatidylcholine. *J. Biol. Chem.* **258**: 4156–4165.
 29. Rider, E. D., M. Ikegami, and A. H. Jobe. 1992. Localization of alveolar surfactant clearance in rabbit lung cells. *Am. J. Physiol.* **263**: L201–L209.
 30. Patterson, B. W., B. Mittendorfer, N. Elias, R. Satyanarayana, and S. Klein. 2002. Use of stable isotopically labeled tracers to measure very low density lipoprotein-triglyceride turnover. *J. Lipid Res.* **43**: 223–233.